

CRYSTALLOGRAPHIC
COMMUNICATIONS

ISSN 2056-9890

Received 15 January 2016

Accepted 16 January 2016

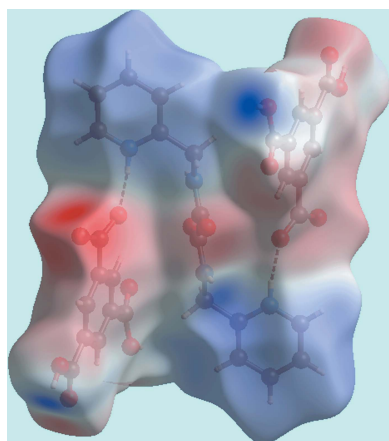
Edited by W. T. A. Harrison, University of
Aberdeen, Scotland† Additional correspondence author, e-mail:
mmjotani@rediffmail.com.**Keywords:** crystal structure; salt; hydrogen
bonding; carboxylate; diamide; Hirshfeld
surface analysis**CCDC reference:** 1447965**Supporting information:** this article has
supporting information at journals.iucr.org/e

2-([[(Pyridin-1-ium-2-ylmethyl)carbamoyl]form- amido}methyl)pyridin-1-ium bis(3,5-dicarboxy- benzoate): crystal structure and Hirshfeld surface analysis

Mukesh M. Jotani,^{a†} Sabrina Syed,^b Siti Nadiyah Abdul Halim^b and Edward R. T.
Tiekink^{c*}

^aDepartment of Physics, Bhavan's Sheth R. A. College of Science, Ahmedabad, Gujarat 380 001, India, ^bDepartment of
Chemistry, University of Malaya, 50603 Kuala Lumpur, Malaysia, and ^cCentre for Crystalline Materials, Faculty of Science
and Technology, Sunway University, 47500 Bandar Sunway, Selangor Darul Ehsan, Malaysia. *Correspondence e-mail:
edwardt@sunway.edu.my

The asymmetric unit of the title salt, $C_{14}H_{16}N_4O_2^{2+} \cdot 2C_9H_5O_6^-$, comprises half a dication, being located about a centre of inversion, and one anion, in a general position. The central $C_4N_2O_2$ group of atoms in the dication are almost planar (r.m.s. deviation = 0.009 Å), and the carbonyl groups lie in an *anti* disposition to enable the formation of intramolecular amide-N—H...O(carbonyl) hydrogen bonds. To a first approximation, the pyridinium and amide N atoms lie to the same side of the molecule [$N_{py}-C-C-N_{amide}$ torsion angle = 34.8 (2)°], and the *anti* pyridinium rings are approximately perpendicular to the central part of the molecule [dihedral angle = 68.21 (8)°]. In the anion, one carboxylate group is almost coplanar with the ring to which it is connected [$C_{ben}-C_{ben}-C_q-O$ torsion angle = 2.0 (3)°], whereas the other carboxylate and carboxylic acid groups are twisted out of the plane [torsion angles = 16.4 (3) and 15.3 (3)°, respectively]. In the crystal, anions assemble into layers parallel to (10 $\bar{4}$) via hydroxy-O—H...O(carbonyl) and charge-assisted hydroxy-O—H...O(carboxylate) hydrogen bonds. The dications are linked into supra-molecular tapes by amide-N—H...O(amide) hydrogen bonds, and thread through the voids in the anionic layers, being connected by charge-assisted pyridinium-N—O(carboxylate) hydrogen bonds, so that a three-dimensional architecture ensues. An analysis of the Hirshfeld surface points to the importance of O—H...O hydrogen bonding in the crystal structure.



1. Chemical context

Of the isomeric *N,N'*-bis(pyridin-*n*-ylmethyl)ethanediamides, *n* = 2, 3 or 4, the molecule with *n* = 2 appears to have attracted the least attention in co-crystallization studies; for the chemical structure of the diprotonated form of the *n* = 2 isomer see Scheme 1. By contrast, the *n* = 3 and 4 molecules have attracted interest from the crystal engineering community in terms of their ability to form co-crystals with iodo-containing species leading to aggregates featuring N...I halogen bonding (Goroff *et al.*, 2005; Jin *et al.*, 2013) as well as carboxylic acids (Nguyen *et al.*, 2001). It is the latter that has formed the focus of our interest in co-crystallization experiments of these molecules which has led to the characterization of both co-crystals (Arman, Kaulgud *et al.*, 2012; Arman, Miller *et al.*, 2012) and salts (Arman *et al.*, 2013). It was during the course of recent studies in this area (Syed *et al.*, 2016) that the title salt was isolated from the 1:1 co-crystallization experiment between the *n* = 2 isomer and trimesic acid. The

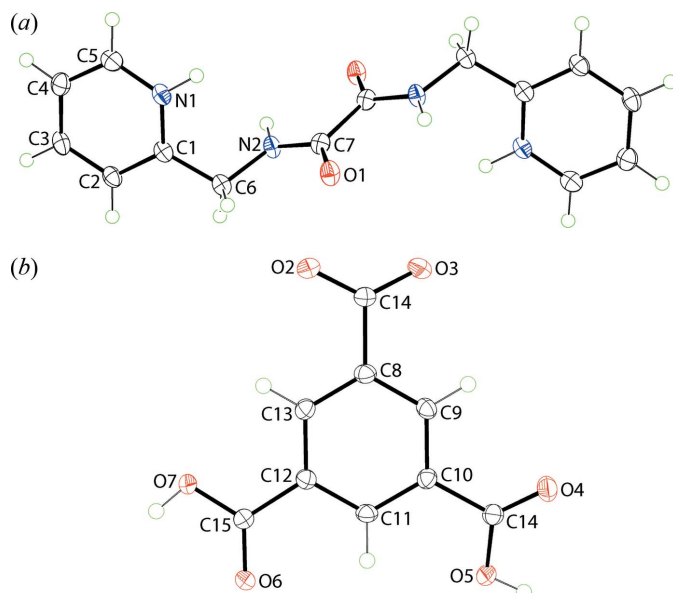
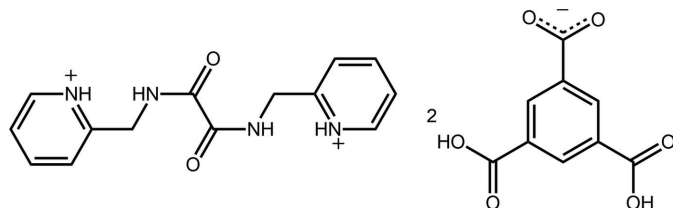


Figure 1

The molecular structures of the ions comprising the title salt, showing the atom-labelling scheme and displacement ellipsoids at the 50% probability level: (a) 2-[[[(pyridin-1-ium-2-ylmethyl)carbamoyl]formamido]methyl]pyridin-1-ium, and (b) 3,5-dicarboxybenzoate; unlabelled atoms are related by the symmetry operation $-x, 1-y, 1-z$.

crystal and molecular structures as well as a Hirshfeld surface analysis of this salt is described herein.



2. Structural commentary

The title salt, Fig. 1, was prepared from the 1:1 reaction of trimesic acid and *N,N'*-bis(pyridin-2-ylmethyl)ethanediamide conducted in ethanol. The harvested crystals were shown by crystallography to comprise (2-pyridinium) $\text{CH}_2\text{N}(\text{H})\text{C}(=\text{O})\text{C}(=\text{O})\text{CH}_2\text{N}(\text{H})(2\text{-pyridinium})$ dications and 3,5-dicarboxybenzoate anions in the ratio 1:2; as the dication is located about a centre of inversion, one anion is found in the asymmetric unit. The confirmation for the transfer of protons

Table 2

Hydrogen-bond geometry (\AA , $^\circ$).

$D-H\cdots A$	$D-H$	$H\cdots A$	$D\cdots A$	$D-H\cdots A$
$\text{N2}-\text{H2N}\cdots\text{O1}^{\text{i}}$	0.88 (2)	2.38 (2)	2.704 (2)	102 (1)
$\text{O7}-\text{H7O}\cdots\text{O6}^{\text{ii}}$	0.85 (2)	1.77 (2)	2.614 (2)	178 (2)
$\text{O5}-\text{H5O}\cdots\text{O2}^{\text{iii}}$	0.85 (2)	1.69 (2)	2.5352 (19)	175 (2)
$\text{N2}-\text{H2N}\cdots\text{O1}^{\text{iv}}$	0.88 (2)	2.01 (2)	2.816 (2)	153 (2)
$\text{N1}-\text{H1N}\cdots\text{O3}^{\text{v}}$	0.89 (2)	1.73 (2)	2.604 (2)	169 (2)
$\text{C5}-\text{H5}\cdots\text{O4}^{\text{vi}}$	0.95	2.46	3.019 (3)	117
$\text{C6}-\text{H6A}\cdots\text{O4}^{\text{vi}}$	0.99	2.55	3.362 (3)	140
$\text{C2}-\text{H2}\cdots\text{O2}^{\text{i}}$	0.95	2.50	3.251 (3)	136
$\text{C3}-\text{H3}\cdots\text{O6}^{\text{vii}}$	0.95	2.59	3.068 (2)	112

Symmetry codes: (i) $-x, -y+1, -z+1$; (ii) $-x, -y+1, -z$; (iii) $-x+2, y+\frac{1}{2}, -z+\frac{1}{2}$; (iv) $x-1, y, z$; (v) $-x+1, -y+1, -z+1$; (vi) $x-2, y, z$; (vii) $x-1, -y+\frac{3}{2}, z+\frac{1}{2}$.

during the co-crystallization experiment is found in (i) the pattern of hydrogen-bonding interactions as discussed in *Supramolecular features*, and (ii) the geometric characteristics of the ions. Thus, the $\text{C}-\text{N}-\text{C}$ angle in the pyridyl ring has expanded by over 3° *cf.* that found in the only neutral form of *N,N'*-bis(pyridin-2-ylmethyl)ethanediamide characterized crystallographically in an all-organic molecule, *i.e.* in a 1:2 co-crystal with 2-aminobenzoic acid (Arman, Miller *et al.*, 2012), Table 1. The observed angle is in agreement with the sole example of a diprotonated form of the molecule, *i.e.* in a 1:2 salt with 2,6-dinitrobenzoate (Arman *et al.*, 2013), Table 1. Further, the experimental equivalence of the $\text{C14}-\text{O2}$, O3 bond lengths, *i.e.* 1.259 (2) and 1.250 (2) \AA is consistent with deprotonation and the formation of a carboxylate group, and contrasts the great disparity in the $\text{C15}-\text{O4}$, O5 [1.206 (2) and 1.320 (2) \AA] and $\text{C16}-\text{O6}$, O7 [1.229 (2) and 1.315 (2) \AA] bond lengths.

In the dication, the central $\text{C}_4\text{N}_2\text{O}_2$ chromophore is almost planar, having an r.m.s. deviation of 0.009 \AA and, from symmetry, the carbonyl groups are *anti*. An intramolecular amide- $\text{N}-\text{H}\cdots\text{O}(\text{carbonyl})$ hydrogen bond is noted, Table 2. The pyridinium- N1 and amide- N2 atoms are approximately *syn* as seen in the value of the $\text{N1}-\text{C1}-\text{C6}-\text{N2}$ torsion angle of $34.8 (2)^\circ$. This planarity does not extend to the terminal pyridinium rings which are approximately perpendicular to and lying to either side of the central chromophore, forming dihedral angles of $68.21 (8)^\circ$. The central $\text{C7}-\text{C7}^{\text{i}}$ bond length of 1.538 (4) \AA is considered long for a $\text{C}-\text{C}$ bond involving sp^2 -hybridized atoms (Spek, 2009). Geometric data for the two previously characterized molecules (Arman, Miller *et al.*, 2012; Arman *et al.*, 2013) related to the dication are collected in Table 1. To a first approximation, the three molecules present the same features as described above with the notable

Table 1

Selected geometric details (\AA , $^\circ$) for an *N,N'*-bis(pyridin-2-ylmethyl)ethanediamide molecule and protonated forms^a.

Cofomer	$\text{C}-\text{N}_{\text{py}}-\text{C}$	$\text{C}_4\text{N}_2\text{O}_2/\text{N-ring}$	$\text{C}(=\text{O})-\text{C}(=\text{O})$	$\text{N}_{\text{py}}-\text{C}-\text{C}-\text{N}_{\text{amide}}$	Refcode ^b	Ref.
$2\text{-NH}_2\text{C}_6\text{H}_4\text{CO}_2\text{H}^{\text{c}}$	119.01 (11)	69.63 (6)	1.54119 (16)	165.01 (10)	DIDZEX	Arman, Miller <i>et al.</i> (2012)
$2,6\text{-(NO}_2)_2\text{C}_6\text{H}_3\text{CO}_2^{\text{-d}}$	123.00 (12)	72.92 (5)	1.5339 (18)	73.84 (15)	TIPHEH	Arman <i>et al.</i> (2013)
$3,5\text{-(CO}_2\text{H)}_2\text{C}_6\text{H}_3\text{CO}_2^{\text{-}}$	122.36 (18)	68.21 (8)	1.538 (3)	34.8 (2)	—	This work

Notes: (a) All diamide molecules/dianions are centrosymmetric; (b) Groom & Allen (2014); (c) 1:2 co-crystal with 2-aminobenzoic acid; (d) 1:2 salt with 2,6-dinitrobenzoate in which both pyridyl-N atoms are protonated.

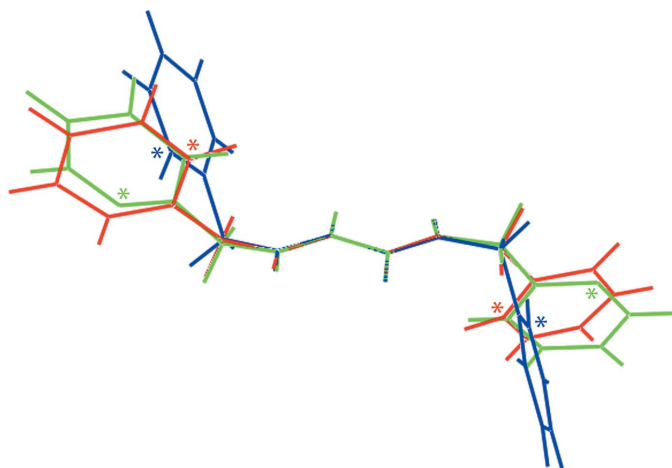


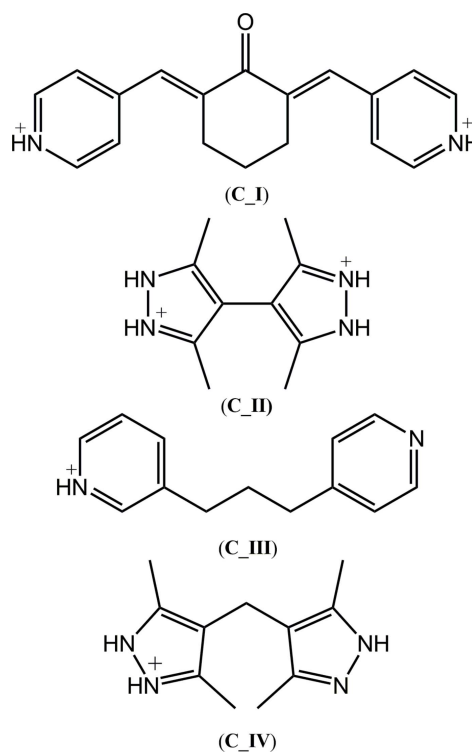
Figure 2

Overlay diagram of the dication in the title compound (red image), the neutral molecule in its co-crystal (green), and dication in the literature salt (blue). The molecules have been overlapped so that the O=C—C=O residues are coincident. The ring N atoms are indicated by an asterisk.

exception of the relative disposition of the pyridinium-N1 and amide-N2 atoms. Thus, in the neutral form of the molecule, these are *anti*, the N1—C1—C6—N2 torsion angle being 165.01 (10)°, and almost perpendicular in the salt, with N1—C1—C6—N2 being 73.84 (15)°. These differences are highlighted in the overlay diagram shown in Fig. 2.

In the anion, the C13—C8—C14—O2 and C9—C10—C15—O4 torsion angles of 15.3 (3) and 16.4 (3)°, respectively, indicate twisted conformations between these residues and the ring to which they are attached whereas the C11—C12—C16—O6 torsion angle of 2.0 (3)° shows this carboxylic acid group to be co-planar with the ring. The conformational flexibility in 3,5-dicarboxybenzoate anions is well illustrated in arguably the four most closely related structures in the crystallographic literature (Groom & Allen, 2014), identified from approximately 35 organic salts containing this anion. Referring to Scheme 2, the most closely related structure features the dication C_I with two protonated pyridyl N atoms (Santra *et al.*, 2009). Here, with two crystallographically independent anions, twists are noted from the mean-plane data collated in Table 3. For one anion, all groups are twisted out of the least-squares plane through the benzene ring but, in the second anion, the carboxylate group is effectively co-planar with the

ring with up to a large twist noted for one of the carboxylic acid groups. In the other example with a diprotonated cation, C_II (Singh *et al.*, 2015), both independent anions exhibit twists of less than 8° with all three residues effectively co-planar in one of the anions. In the example with a single protonated pyridyl residue, C_III (Ferguson *et al.*, 1998), twists are evident for one of the carboxylic acid groups and for the carboxylate but, the second carboxylic acid residue is effectively co-planar. Finally, in the mono-protonated species related to C_I, *i.e.* C_IV (Basu *et al.*, 2009), twists are evident for all groups with the maximum twists observed in the series for the carboxylate residue, *i.e.* 25.13 (10)°, and for one of the carboxylic acid groups, *i.e.* 22.50 (10)°.



3. Supramolecular features

The molecular packing may be conveniently described in terms of O—H...O hydrogen bonding to define an anionic network which is connected into a three-dimensional architecture by N—H...O hydrogen bonds; Table 2 collates geometric data for the intermolecular interactions discussed in

Table 3

Dihedral angles (°) for the 3,5-dicarboxybenzoate anion in the title salt and in selected literature precedents^a.

Cation	C ₆ /CO ₂	C ₆ /CO ₂ H	C ₆ /CO ₂ H	CSD Refcode ^b	Ref.
C_I ^c	8.6 (2) 1.6 (2)	4.96 (19) 8.9 (2)	12.82 (16) 19.13 (15)	QUFYIA	Santra <i>et al.</i> (2009)
C_II ^c	4.5 (3) 2.1 (4)	7.5 (4) 2.0 (4)	3.43 (18) 2.6 (3)	LUBJAV	Singh <i>et al.</i> (2015)
C_III	5.92 (11)	1.69 (14)	10.38 (10)	NIFGOY	Ferguson <i>et al.</i> (1998)
C_IV	25.13 (10)	22.50 (10)	11.60 (7)	CUMQUX	Basu <i>et al.</i> (2009)
dication	15.70 (13)	16.34 (12)	1.99 (10)	—	This work

Notes: (a) Refer to Scheme 2 for chemical structures; (b) Groom & Allen (2014); (c) Two independent anions.

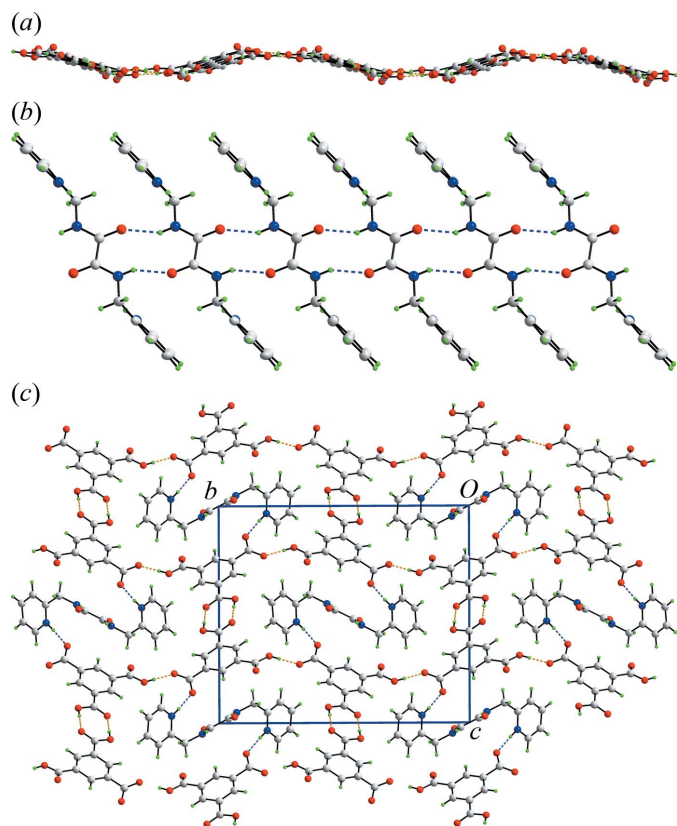


Figure 3

Molecular packing in the title salt: (a) supramolecular layers mediated by O—H...O hydrogen bonds, (b) supramolecular tapes mediated by N—H...O hydrogen bonds, and (c) a view of the unit-cell contents shown in projection down the *a* axis, whereby the supramolecular layers, illustrated in Fig. 3(a), are linked by charge-assisted N—H...O(carboxylate) hydrogen bonds to consolidate a three-dimensional architecture. The O—H...O and N—H...O hydrogen bonds are shown as orange and blue dashed lines, respectively.

this section. Thus, centrosymmetrically related C—O6,O7 carboxylic acid groups associate *via* hydroxy-O—H...O(carbonyl) hydrogen bonds to form a familiar eight-membered {...HOCO}₂ synthon. These are connected by charge-assisted hydroxy-O—H...O(carboxylate) hydrogen bonds that form C(8) chains. The result is a network of anions lying parallel to (10 $\bar{4}$) and having an undulating topology, Fig. 3a. The dications also self-associate to form supramolecular tapes *via* C(4) chains featuring pairs of amide-N—H...O(amide) hydrogen bonds and 10-membered {...HNC₂O}₂ synthons, Fig. 3b. The tapes are aligned along the *a* axis and, in essence, thread through the voids in the anionic layers to form a three-dimensional architecture, Fig. 3c. The links between the anionic layers and cationic tapes are hydrogen bonds of the type charge-assisted pyridinium-N—O(carboxylate). In this scheme, no apparent role for the carbonyl-O4 atom is evident. However, this atom accepts two C—H...O interactions from pyridyl- and methylene-H to consolidate the molecular packing. Additional stabilization is afforded by pyridyl-C—H...O(carboxylate, carbonyl) interactions, Table 2.

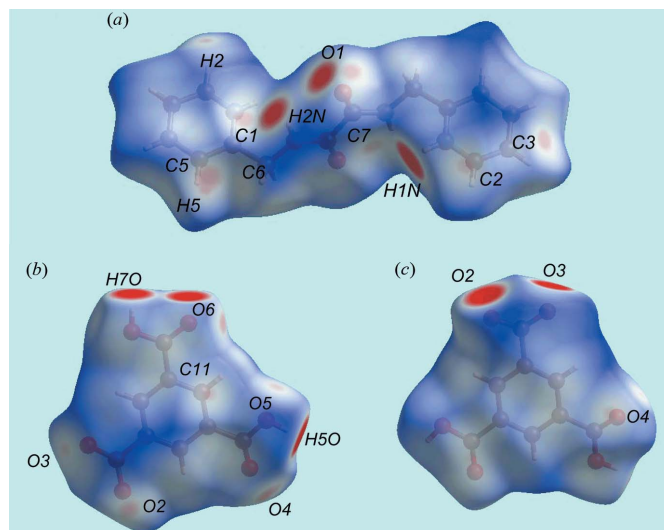


Figure 4

Views of the Hirshfeld surface mapped over d_{norm} in the title salt: (a) dication, (b) and (c) anion.

4. Analysis of the Hirshfeld surfaces

Crystal Explorer 3.1 (Wolff *et al.*, 2012) was used to generate Hirshfeld surfaces (Spackman & Jayatilaka, 2009) mapped over d_{norm} , d_e and electrostatic potential for the title salt. The electrostatic potentials were calculated using *TONTO* (Spackman *et al.*, 2008; Jayatilaka *et al.*, 2005) integrated with

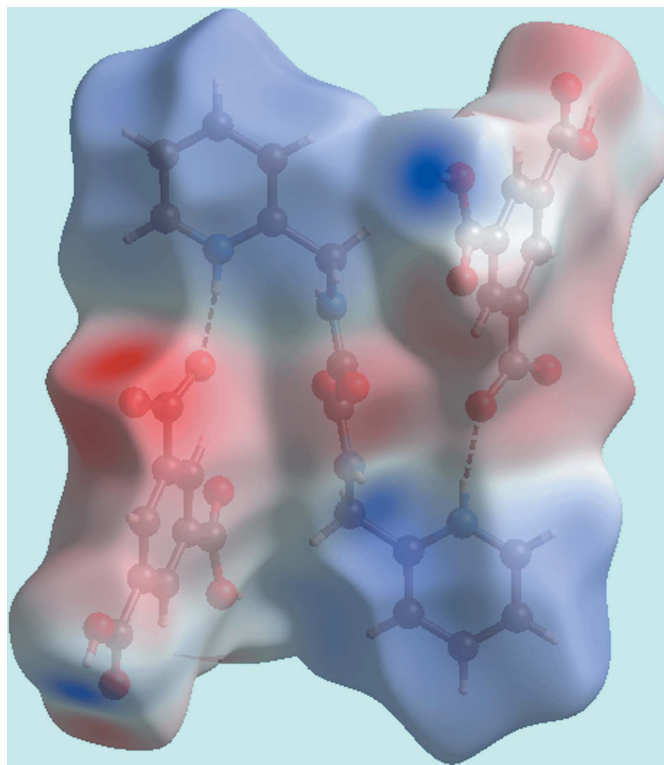


Figure 5

View of the Hirshfeld surface mapped over the calculated electrostatic potential of the tri-ion aggregate in the title salt.

Table 4
Short interatomic contacts (Å) in the title salt.

Contact	Distance	Symmetry operation
C1...O1	3.096 (2)	$-1 + x, y, z$
C7...O3	3.072 (3)	$1 - x, 1 - y, 1 - z$
C11...O4	3.141 (3)	$-1 + x, y, z$
C14...H1N	2.74 (2)	$1 - x, 1 - y, 1 - z$
C10...H6A	2.77	$1 + x, y, z$
C14...H5O	2.631 (17)	$-x, -\frac{1}{2} + y, \frac{1}{2} - z$
C16...H7O	2.70 (2)	$-x, 1 - y, -z$

Table 5
Percentage contribution of the different intermolecular interactions to the Hirshfeld surfaces for the dication, anion and salt.

Contact	Dication	Anion	Salt
O...H/H...O	41.6	47.2	43.2
H...H	25.1	16.7	23.7
C...H/H...C	20.2	17.4	17.3
C...O/O...C	6.6	12.8	10.2
N...H/H...N	2.3	0.3	1.1
C...C	0.2	3.0	2.2
O...O	1.2	2.0	1.0
N...O/O...N	2.3	0.1	1.2
N...C/C...N	0.5	0.5	0.1

Crystal Explorer, and mapped on the Hirshfeld surfaces using the STO-3G basis set at the Hartree–Fock level theory over the range ± 0.25 au. The contact distances d_i and d_e from the Hirshfeld surface to the nearest atom inside and outside, respectively, enable the analysis of the intermolecular interactions through the mapping of d_{norm} . The combination of d_e and d_i in the form of two-dimensional fingerprint plots provides a summary of intermolecular contacts in the crystal (Rohl *et al.*, 2008).

Views of the Hirshfeld surface mapped over d_{norm} in the title salt are given in Fig. 4. The formation of charge-assisted hydroxyl-O—H...O(carboxylate) and pyridinium-N—H...O(carboxylate) hydrogen bonds in the crystal appear as distinct dark-red spots near the respective donor and acceptor atoms. In Fig. 5, the blue and red colouration are the corresponding regions on the surface mapped over the electrostatic potential. The dark-red spots on the Hirshfeld surface of the dication corresponds to a pair of amide-N—H...O(amide) hydrogen bonds leading to the supramolecular tape. Intermolecular C—H...O and N—H...O interactions, representing weak hydrogen bonds over and above those discussed above in *Supramolecular features*, result in light-red spots near some of the carbon, nitrogen and oxygen atoms, Fig. 4. Hence, the contribution to the surface from these interactions involve not only O...H/H...O contacts but also C...O/O...C and N...O/O...N contacts, Table 4. The relative contributions of the different contacts to the Hirshfeld surfaces are collated in Table 5 for the entire structure and also delineated for the dication and anion. The linkage of ions through the formation of hydrogen bonds is illustrated in Fig. 6.

The overall two-dimensional fingerprint plot (FP) of the salt together with those of the dication and anion, and FP's delineated into H...H, O...H/H...O, C...H/H...C and

C...O/O...C contacts are illustrated in Fig. 7. The O...H/H...O contacts have the largest overall contribution to the Hirshfeld surface, *i.e.* 43.2%, and these interactions dominate in the crystal structure. The prominent spike with green points appearing in the lower left region in the FP for the anion at $d_e + d_i \sim 1.7$ Å has a major contribution, *i.e.* 47.2%, from O...H contacts; the spike at the same $d_e + d_i$ distance is due to a small contribution, 10.0%, from H...O contacts. The different contributions from O...H and H...O contacts to the Hirshfeld surface of the dication, *i.e.* 6.8 and 34.8%, respectively, lead to asymmetric peaks at $d_e + d_i \sim 1.8$ and 2.0 Å, respectively, indicating the varying strength of these interactions. However, the overall FP of the salt delineated into O...H/H

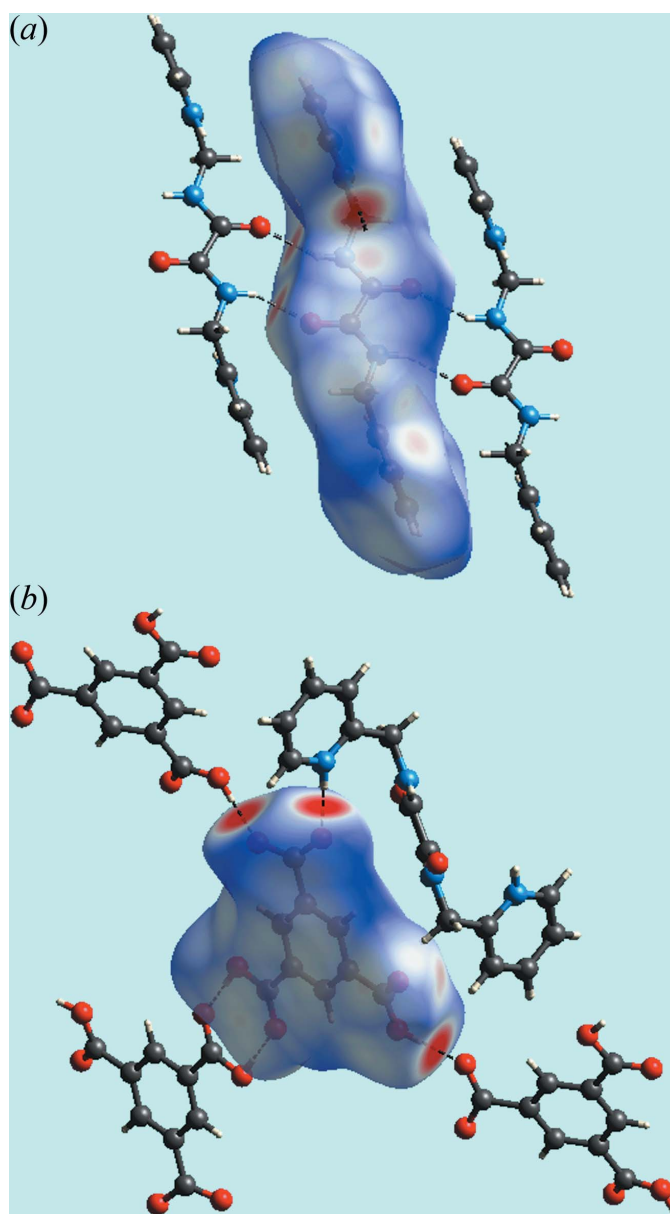


Figure 6
Views of the Hirshfeld surfaces mapped over d_{norm} in the title salt emphasizing the interactions between (a) dianions and (b) the environment about the anion.

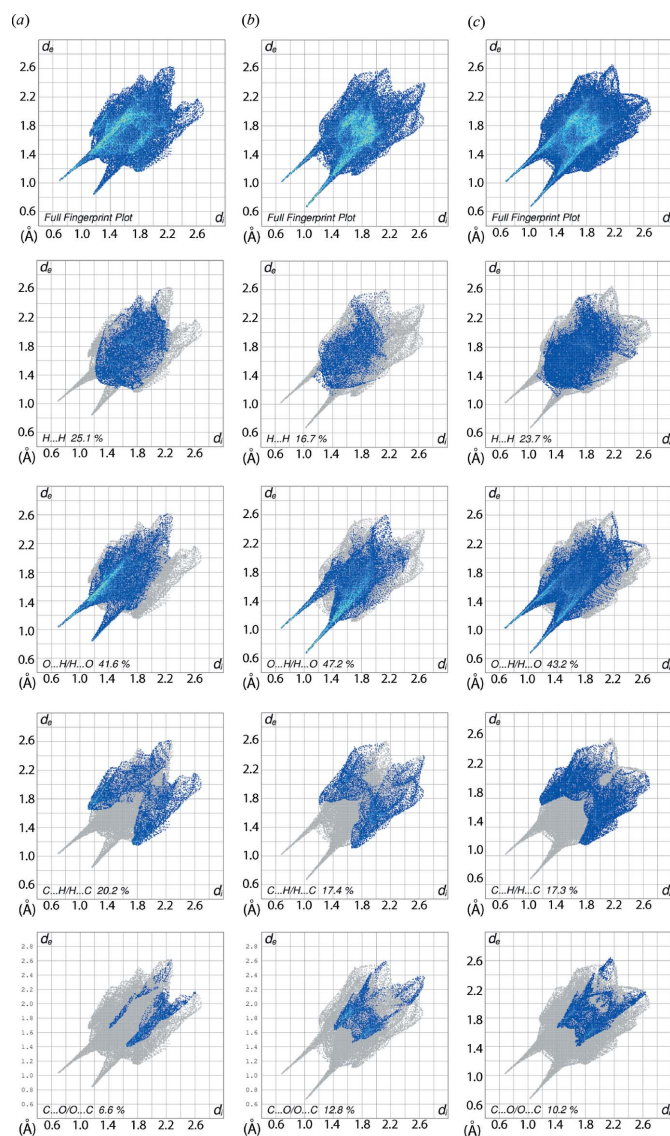


Figure 7

The two-dimensional fingerprint plots for the title salt: (a) dication, (b) anion, and (c) full structure, showing contributions from different contacts, *i.e.* $\text{H}\cdots\text{H}$, $\text{O}\cdots\text{H}/\text{H}\cdots\text{O}$, $\text{C}\cdots\text{H}/\text{H}\cdots\text{C}$, and $\text{C}\cdots\text{O}/\text{O}\cdots\text{C}$.

$\text{H}\cdots\text{O}$ contacts shows a symmetric pair of spikes at $d_e + d_i \sim 1.7$ Å with nearly equal contributions from $\text{O}\cdots\text{H}$ and $\text{H}\cdots\text{O}$ contacts. A smaller contribution is made by the $\text{H}\cdots\text{H}$ contacts, Table 1, and these appear as the scattered points without a distinct peak, Fig. 7. The presence of short interatomic $\text{C}\cdots\text{H}/\text{H}\cdots\text{C}$ contacts, Table 4, result in a 17.3% overall contribution to the surface, although there are no $\text{C}-\text{H}\cdots\pi$ contacts within the acceptance distance criteria for such interactions (Spek, 2009). These are represented by a pair of symmetrical wings at $d_e + d_i \sim 2.9$ Å in the FP plot, Fig. 7. The contribution from $\text{C}\cdots\text{O}/\text{O}\cdots\text{C}$ contacts to the Hirshfeld surface is also evident from the presence of intermolecular $\text{C}-\text{H}\cdots\text{O}$ interactions as well as short interatomic $\text{C}\cdots\text{O}/\text{O}\cdots\text{C}$ contact, Table 4. These appear as cross-over wings in the (d_e, d_i) region between 1.7 and 2.7 Å. A small but significant contribution to the Hirshfeld surface of the dication due

Table 6

Enrichment ratios (ER) for the dication, anion and salt.

Contact	Dication	Anion	Salt
$\text{O}\cdots\text{H}/\text{H}\cdots\text{O}$	1.37	1.50	1.40
$\text{H}\cdots\text{H}$	0.77	0.69	0.80
$\text{C}\cdots\text{H}/\text{H}\cdots\text{C}$	1.27	0.96	0.99
$\text{C}\cdots\text{O}/\text{O}\cdots\text{C}$	0.90	1.09	1.13
$\text{N}\cdots\text{H}/\text{H}\cdots\text{N}$	0.77	0.68	0.88
$\text{N}\cdots\text{O}/\text{O}\cdots\text{N}$	1.68	—	—

to $\text{N}\cdots\text{O}/\text{O}\cdots\text{N}$ contacts is the result of intermolecular amide- $\text{N}-\text{H}\cdots\text{O}$ (amide) interactions.

The intermolecular interactions were further analysed using a recently reported descriptor, the enrichment ratio, ER (Jelsch *et al.*, 2014), which is based on Hirshfeld surface analysis and gives an indication of the relative likelihood of specific intermolecular interactions to form; the calculated ratios are given in Table 6. The relatively poor content of hydrogen atoms in the salt and the involvements of many hydrogen atoms in the intermolecular interactions, as discussed above, reduces the ER value of non-bonded $\text{H}\cdots\text{H}$ contacts to a value less unity, *i.e.* 0.8, due to a 23.7% contribution from the 54.5% available Hirshfeld surface and anticipated 29.7% random contacts. The ER value of 1.4 corresponding to $\text{O}\cdots\text{H}/\text{H}\cdots\text{O}$ contacts results from a relatively high 43.2% contribution by $\text{O}-\text{H}\cdots\text{O}$, $\text{N}-\text{H}\cdots\text{O}$ and $\text{C}-\text{H}\cdots\text{O}$ interactions. The carbon and oxygen atoms involved in the intermolecular $\text{C}-\text{H}\cdots\text{O}$ interactions and short inter $\text{C}\cdots\text{O}/\text{O}\cdots\text{C}$ contacts are at distances shorter than the sum of their respective van der Waals radii, hence they also have a high formation propensity, so the ER value is > 1 . The $\text{C}\cdots\text{H}/\text{H}\cdots\text{C}$ contacts in the crystal are enriched due to the poor nitrogen content and the presence of short interatomic $\text{C}\cdots\text{H}/\text{H}\cdots\text{C}$ contacts so the ratio is close to unity, *i.e.* 0.99. Finally, the ER value of 1.68 corresponding to $\text{N}\cdots\text{O}/\text{O}\cdots\text{N}$ contacts for the surface of dication is the result of the charge-assisted $\text{N}-\text{H}\cdots\text{O}$ interactions consistent with their high propensity to form.

5. Database survey

As mentioned in the *Chemical context*, N,N' -bis(pyridin-2-ylmethyl)ethanediamide (LH_2), has not been as well studied as the $n = 3$ and 4 isomers. This notwithstanding, the coordination chemistry of LH_2 is more advanced and diverse. Thus, co-crystals have been reported with a metal complex, *i.e.* $[\text{Mn}(1,10\text{-phenanthroline})_3][\text{ClO}_4]_2 \cdot (\text{LH}_2)$ (Liu *et al.*, 1999). Monodentate coordination *via* a pyridyl-N atom was found in mononuclear $\text{HgI}_2(\text{LH}_2)_2$ (Zeng *et al.*, 2008). Bidentate, bridging *via* both pyridyl-N atoms has been observed in binuclear $\{[\text{Me}_2(4\text{-HO}_2\text{CC}_6\text{H}_4\text{CH}_2)\text{Pt}(4,4'\text{-di-}i\text{-butyl-}2,2'\text{-bipyridyl})_2(\text{LH}_2)]_2\}^{2+}$ (Fraser *et al.*, 2002) and in a polymeric silver salt, $\{\text{AgBF}_4(\text{LH}_2) \cdot \text{H}_2\text{O}\}_n$ (Schauer *et al.*, 1998). In the analogous triflate salt $\{\text{Ag}_2(\text{O}_3\text{SCF}_3)_2(\text{LH}_2)_3\}_n$ (Arman *et al.*, 2010), one LH_2 bridges as in the BF_4 salt (Schauer *et al.*, 1998) but the other two LH_2 molecules bridge one Ag^+ *via* a pyridyl-N atom and another *via* the second pyridyl-N atom as well as a

Table 7
Experimental details.

Crystal data	
Chemical formula	$C_{14}H_{16}N_4O_2^{2+} \cdot 2C_9H_5O_6^-$
M_r	690.56
Crystal system, space group	Monoclinic, $P2_1/c$
Temperature (K)	100
a, b, c (Å)	5.0436 (3), 18.4232 (10), 16.0796 (9)
β (°)	95.878 (5)
V (Å ³)	1486.25 (15)
Z	2
Radiation type	Mo $K\alpha$
μ (mm ⁻¹)	0.12
Crystal size (mm)	0.30 × 0.10 × 0.05
Data collection	
Diffractometer	Agilent SuperNova Dual diffractometer with an Atlas detector
Absorption correction	Multi-scan (<i>CrysAlis PRO</i> ; Agilent, 2014)
T_{min}, T_{max}	0.580, 1.000
No. of measured, independent and observed [$I > 2\sigma(I)$] reflections	17686, 3410, 2656
R_{int}	0.069
$(\sin \theta/\lambda)_{max}$ (Å ⁻¹)	0.650
Refinement	
$R[F^2 > 2\sigma(F^2)], wR(F^2), S$	0.051, 0.134, 1.07
No. of reflections	3410
No. of parameters	238
No. of restraints	4
$\Delta\rho_{max}, \Delta\rho_{min}$ (e Å ⁻³)	0.46, -0.26

Computer programs: *CrysAlis PRO* (Agilent, 2014), *SHELXS97* (Sheldrick, 2008), *SHELXL2014* (Sheldrick, 2015), *ORTEP-3 for Windows* (Farrugia, 2012), *QMol* (Gans & Shalloway, 2001), *DIAMOND* (Brandenburg, 2006) and *publCIF* (Westrip, 2010).

carbonyl-O atom, *i.e.* are tridentate. In a variation, tetradentate, bridging coordination *via* all four nitrogen atoms is found in polymeric $[CuL(LH_2)(OH_2)]_n$ (Lloret *et al.*, 1989). Deprotonation of LH_2 leads to a tetradentate ligand coordinating *via* all four nitrogen atoms in PdL (Reger *et al.*, 2003). There are several examples of hexadentate- N_4O_2 coordination in copper(II) chemistry, as in the aforementioned $[CuL(LH_2)(OH_2)]_n$ (Lloret *et al.*, 1989) and, for example, in polymeric $[CuL(\mu_2-4,4'-bipyridyl)-(OH_2)]_2$ (Zhang *et al.*, 2001).

6. Synthesis and crystallization

The diamide (0.25 g), prepared in accord with the literature procedure (Schauer *et al.*, 1997), in ethanol (10 ml) was added to a ethanol solution (10 ml) of trimesic acid (Acros Organic, 0.18 g). The mixture was stirred for 2 h at room temperature. After standing for a few minutes, a white precipitate formed which was filtered off by vacuum suction. The filtrate was then left to stand under ambient conditions, yielding pale-yellow crystals after 2 weeks.

7. Refinement

Crystal data, data collection and structure refinement details are summarized in Table 7. The carbon-bound H atoms were

placed in calculated positions ($C-H = 0.95-0.99$ Å) and were included in the refinement in the riding-model approximation, with $U_{iso}(H)$ set to $1.2U_{eq}(C)$. The oxygen- and nitrogen-bound H atoms were located in a difference Fourier map but were refined with distance restraints of $O-H = 0.84 \pm 0.01$ Å and $N-H = 0.88 \pm 0.01$ Å, and with $U_{iso}(H)$ set to $1.5U_{eq}(O)$ and $1.2U_{eq}(N)$.

Acknowledgements

The authors thank the Exploratory Research Grant Scheme (ER008-2013A) for support.

References

- Agilent (2014). *CrysAlis PRO*. Agilent Technologies Inc., Santa Clara, CA, USA.
- Arman, H. D., Miller, T. & Tiekink, E. R. T. (2012). *Z. Kristallogr.* **227**, 825–830.
- Arman, H. D., Kaulgud, T., Miller, T., Poplaukhin, P. & Tiekink, E. R. T. (2012). *J. Chem. Crystallogr.* **42**, 673–679.
- Arman, H. D., Miller, T., Poplaukhin, P. & Tiekink, E. R. T. (2010). *Acta Cryst. E* **66**, m1167–m1168.
- Arman, H. D., Miller, T., Poplaukhin, P. & Tiekink, E. R. T. (2013). *Z. Kristallogr.* **228**, 295–303.
- Basu, T., Sparkes, H. A. & Mondal, R. (2009). *Cryst. Growth Des.* **9**, 5164–5175.
- Brandenburg, K. (2006). *DIAMOND*. Crystal Impact GbR, Bonn, Germany.
- Farrugia, L. J. (2012). *J. Appl. Cryst.* **45**, 849–854.
- Ferguson, G., Glidewell, C., McManus, G. D. & Meehan, P. R. (1998). *Acta Cryst. C* **54**, 418–421.
- Fraser, C. S. A., Eisler, D. J., Jennings, M. C. & Puddephatt, R. J. (2002). *Chem. Commun.* pp. 1224–1225.
- Gans, J. & Shalloway, D. (2001). *J. Mol. Graphics Modell.* **19**, 557–559.
- Goroff, N. S., Curtis, S. M., Webb, J. A., Fowler, F. W. & Lauher, J. W. (2005). *Org. Lett.* **7**, 1891–1893.
- Groom, C. R. & Allen, F. H. (2014). *Angew. Chem. Int. Ed.* **53**, 662–671.
- Jayatilaka, D., Grimwood, D. J., Lee, A., Lemay, A., Russel, A. J., Taylor, C., Wolff, S. K., Cassam-Chenai, P. & Whitton, A. (2005). *TONTO*. Available at: <http://hirshfeldsurface.net/>.
- Jelsch, C., Ejsmont, K. & Huder, L. (2014). *IUCrJ*, **1**, 119–128.
- Jin, H., Plonka, A. M., Parise, J. B. & Goroff, N. S. (2013). *CrystEngComm*, **15**, 3106–3110.
- Liu, B., Wang, H.-M., Yan, S.-P., Liao, D.-Z., Jiang, Z.-H., Huang, X.-Y. & Wang, G.-L. (1999). *J. Chem. Crystallogr.* **29**, 623–627.
- Lloret, F., Julve, M., Faus, J., Journaux, Y., Philoche-Levisalles, M. & Jeannin, Y. (1989). *Inorg. Chem.* **28**, 3702–3706.
- Nguyen, T. L., Fowler, F. W. & Lauher, J. W. (2001). *J. Am. Chem. Soc.* **123**, 11057–11064.
- Reger, D. L., Smith, D. M. C., Shimizu, K. D. & Smith, M. D. (2003). *Acta Cryst. E* **59**, m652–m654.
- Rohl, A. L., Moret, M., Kaminsky, W., Claborn, K., McKinnon, J. J. & Kahr, B. (2008). *Cryst. Growth Des.* **8**, 4517–4525.
- Santra, R. & Biradha, K. (2009). *Cryst. Growth Des.* **9**, 4969–4978.
- Schauer, C. L., Matwey, E., Fowler, F. W. & Lauher, J. W. (1997). *J. Am. Chem. Soc.* **119**, 10245–10246.
- Schauer, C. L., Matwey, E., Fowler, F. W. & Lauher, J. W. (1998). *Cryst. Eng.* **1**, 213–223.
- Sheldrick, G. M. (2008). *Acta Cryst. A* **64**, 112–122.
- Sheldrick, G. M. (2015). *Acta Cryst. C* **71**, 3–8.
- Singh, U. P., Tomar, K. & Kashyap, S. (2015). *CrystEngComm*, **17**, 1421–1433.

- Spackman, M. A. & Jayatilaka, D. (2009). *CrystEngComm*, **11**, 19–32.
- Spackman, M. A., McKinnon, J. J. & Jayatilaka, D. (2008). *CrystEngComm*, **10**, 377–388.
- Spek, A. L. (2009). *Acta Cryst.* **D65**, 148–155.
- Syed, S., Halim, S. N. A., Jotani, M. M. & Tiekink, E. R. T. (2016). *Acta Cryst.* **E72**, 76–82.
- Westrip, S. P. (2010). *J. Appl. Cryst.* **43**, 920–925.
- Wolff, S. K., Grimwood, D. J., McKinnon, J. J., Turner, M. J., Jayatilaka, D. & Spackman, M. A. (2012). *Crystal Explorer*. The University of Western Australia, Australia.
- Zeng, Q., Li, M., Wu, D., Lei, S., Liu, C., Piao, L., Yang, Y., An, S. & Wang, C. (2008). *Cryst. Growth Des.* **8**, 869–876.
- Zhang, H.-X., Kang, B.-S., Zhou, Z.-Y., Chan, A. S. C., Chen, Z.-N. & Ren, C. (2001). *J. Chem. Soc. Dalton Trans.* pp. 1664–1669.

supporting information

Acta Cryst. (2016). E72, 241-248 [doi:10.1107/S2056989016000980]

2-([(Pyridin-1-ium-2-ylmethyl)carbamoyl]formamido)methylpyridin-1-ium bis(3,5-dicarboxybenzoate): crystal structure and Hirshfeld surface analysis

Mukesh M. Jotani, Sabrina Syed, Siti Nadiah Abdul Halim and Edward R. T. Tiekink

Computing details

Data collection: *CrysAlis PRO* (Agilent, 2014); cell refinement: *CrysAlis PRO* (Agilent, 2014); data reduction: *CrysAlis PRO* (Agilent, 2014); program(s) used to solve structure: *SHELXS97* (Sheldrick, 2008); program(s) used to refine structure: *SHELXL2014* (Sheldrick, 2015); molecular graphics: *ORTEP-3 for Windows* (Farrugia, 2012), *QMol* (Gans & Shalloway, 2001) and *DIAMOND* (Brandenburg, 2006); software used to prepare material for publication: *publCIF* (Westrip, 2010).

2-([(Pyridin-1-ium-2-ylmethyl)carbamoyl]formamido)methylpyridin-1-ium bis(3,5-dicarboxybenzoate)

Crystal data

$\text{C}_{14}\text{H}_{16}\text{N}_4\text{O}_2^{2+} \cdot 2\text{C}_9\text{H}_5\text{O}_6^-$

$M_r = 690.56$

Monoclinic, $P2_1/c$

$a = 5.0436$ (3) Å

$b = 18.4232$ (10) Å

$c = 16.0796$ (9) Å

$\beta = 95.878$ (5)°

$V = 1486.25$ (15) Å³

$Z = 2$

$F(000) = 716$

$D_x = 1.543$ Mg m⁻³

Mo $K\alpha$ radiation, $\lambda = 0.71073$ Å

Cell parameters from 6152 reflections

$\theta = 3.4\text{--}29.2^\circ$

$\mu = 0.12$ mm⁻¹

$T = 100$ K

Prism, pale-yellow

$0.30 \times 0.10 \times 0.05$ mm

Data collection

Agilent SuperNova Dual

diffractometer with an Atlas detector

Radiation source: SuperNova (Mo) X-ray

Source

Mirror monochromator

Detector resolution: 10.4041 pixels mm⁻¹

ω scan

Absorption correction: multi-scan

(*CrysAlis PRO*; Agilent, 2014)

$T_{\min} = 0.580$, $T_{\max} = 1.000$

17686 measured reflections

3410 independent reflections

2656 reflections with $I > 2\sigma(I)$

$R_{\text{int}} = 0.069$

$\theta_{\max} = 27.5^\circ$, $\theta_{\min} = 3.4^\circ$

$h = -6 \rightarrow 6$

$k = -23 \rightarrow 23$

$l = -20 \rightarrow 20$

Refinement

Refinement on F^2

Least-squares matrix: full

$R[F^2 > 2\sigma(F^2)] = 0.051$

$wR(F^2) = 0.134$

$S = 1.07$

3410 reflections

238 parameters

4 restraints

Hydrogen site location: mixed

$w = 1/[\sigma^2(F_o^2) + (0.0563P)^2 + 0.8519P]$

where $P = (F_o^2 + 2F_c^2)/3$

$(\Delta/\sigma)_{\max} < 0.001$

$\Delta\rho_{\max} = 0.46$ e Å⁻³

$\Delta\rho_{\min} = -0.26$ e Å⁻³

Special details

Geometry. All esds (except the esd in the dihedral angle between two l.s. planes) are estimated using the full covariance matrix. The cell esds are taken into account individually in the estimation of esds in distances, angles and torsion angles; correlations between esds in cell parameters are only used when they are defined by crystal symmetry. An approximate (isotropic) treatment of cell esds is used for estimating esds involving l.s. planes.

Fractional atomic coordinates and isotropic or equivalent isotropic displacement parameters (\AA^2)

	<i>x</i>	<i>y</i>	<i>z</i>	$U_{\text{iso}}^*/U_{\text{eq}}$
O1	0.2441 (3)	0.56058 (7)	0.47153 (9)	0.0231 (3)
N1	−0.3956 (3)	0.69095 (9)	0.53385 (11)	0.0198 (4)
H1N	−0.285 (4)	0.6629 (11)	0.5665 (12)	0.024*
N2	−0.2089 (3)	0.56875 (9)	0.45086 (11)	0.0194 (4)
H2N	−0.364 (3)	0.5516 (12)	0.4615 (14)	0.023*
C1	−0.3894 (4)	0.69266 (10)	0.45027 (12)	0.0187 (4)
C2	−0.5582 (4)	0.73355 (11)	0.57322 (13)	0.0226 (4)
H2	−0.5589	0.7300	0.6321	0.027*
C3	−0.7242 (4)	0.78235 (11)	0.52887 (13)	0.0241 (4)
H3	−0.8446	0.8113	0.5562	0.029*
C4	−0.7117 (4)	0.78821 (11)	0.44357 (13)	0.0234 (4)
H4	−0.8184	0.8231	0.4122	0.028*
C5	−0.5438 (4)	0.74330 (10)	0.40389 (13)	0.0209 (4)
H5	−0.5349	0.7472	0.3453	0.025*
C6	−0.2190 (4)	0.63885 (10)	0.40966 (13)	0.0208 (4)
H6A	−0.2906	0.6325	0.3504	0.025*
H6B	−0.0358	0.6584	0.4107	0.025*
C7	0.0204 (4)	0.53666 (11)	0.47870 (12)	0.0197 (4)
O2	0.8690 (3)	0.32072 (7)	0.27064 (9)	0.0253 (3)
O3	1.1233 (3)	0.39299 (8)	0.35861 (9)	0.0298 (4)
O4	1.2729 (3)	0.64690 (8)	0.25738 (10)	0.0260 (3)
O5	0.9119 (3)	0.69980 (7)	0.19086 (9)	0.0243 (3)
H5O	0.994 (5)	0.7391 (9)	0.2034 (16)	0.036*
O6	0.2374 (3)	0.55161 (7)	0.03570 (9)	0.0220 (3)
O7	0.1837 (3)	0.43588 (7)	0.07250 (9)	0.0217 (3)
H7O	0.049 (3)	0.4407 (14)	0.0370 (13)	0.033*
C8	0.8550 (4)	0.44714 (10)	0.24689 (12)	0.0183 (4)
C9	0.9905 (4)	0.51294 (10)	0.25715 (12)	0.0178 (4)
H9	1.1439	0.5167	0.2964	0.021*
C10	0.9018 (4)	0.57340 (10)	0.20997 (12)	0.0171 (4)
C11	0.6784 (4)	0.56752 (10)	0.15260 (12)	0.0180 (4)
H11	0.6170	0.6086	0.1205	0.022*
C12	0.5438 (4)	0.50196 (10)	0.14184 (12)	0.0178 (4)
C13	0.6305 (4)	0.44181 (10)	0.18970 (12)	0.0180 (4)
H13	0.5360	0.3972	0.1832	0.022*
C14	0.9579 (4)	0.38131 (10)	0.29671 (12)	0.0197 (4)
C15	1.0500 (4)	0.64353 (10)	0.22231 (12)	0.0191 (4)
C16	0.3081 (4)	0.49865 (10)	0.07891 (12)	0.0184 (4)

Atomic displacement parameters (\AA^2)

	U^{11}	U^{22}	U^{33}	U^{12}	U^{13}	U^{23}
O1	0.0151 (7)	0.0200 (7)	0.0337 (8)	−0.0005 (5)	−0.0001 (6)	0.0019 (6)
N1	0.0211 (9)	0.0166 (8)	0.0204 (9)	−0.0001 (6)	−0.0033 (7)	0.0019 (7)
N2	0.0166 (8)	0.0145 (8)	0.0264 (9)	0.0000 (6)	−0.0006 (7)	0.0020 (7)
C1	0.0193 (9)	0.0160 (9)	0.0197 (10)	−0.0030 (7)	−0.0031 (7)	0.0000 (8)
C2	0.0266 (11)	0.0206 (10)	0.0197 (10)	−0.0036 (8)	−0.0014 (8)	−0.0006 (8)
C3	0.0276 (11)	0.0176 (10)	0.0272 (11)	−0.0007 (8)	0.0027 (8)	−0.0034 (8)
C4	0.0274 (11)	0.0145 (9)	0.0270 (11)	0.0008 (8)	−0.0032 (8)	0.0008 (8)
C5	0.0252 (10)	0.0166 (9)	0.0201 (10)	−0.0018 (8)	−0.0024 (8)	0.0006 (8)
C6	0.0221 (10)	0.0176 (10)	0.0221 (10)	−0.0002 (7)	−0.0006 (8)	0.0021 (8)
C7	0.0188 (9)	0.0191 (10)	0.0207 (10)	−0.0003 (7)	−0.0002 (7)	−0.0034 (8)
O2	0.0290 (8)	0.0153 (7)	0.0298 (8)	0.0007 (6)	−0.0060 (6)	0.0020 (6)
O3	0.0359 (9)	0.0218 (8)	0.0281 (8)	0.0010 (6)	−0.0140 (7)	0.0031 (6)
O4	0.0214 (7)	0.0204 (7)	0.0341 (9)	−0.0014 (6)	−0.0071 (6)	−0.0030 (6)
O5	0.0260 (8)	0.0135 (7)	0.0313 (8)	−0.0026 (6)	−0.0074 (6)	0.0017 (6)
O6	0.0220 (7)	0.0185 (7)	0.0234 (7)	−0.0015 (5)	−0.0072 (6)	0.0036 (6)
O7	0.0210 (7)	0.0163 (7)	0.0256 (8)	−0.0035 (5)	−0.0084 (6)	0.0020 (6)
C8	0.0220 (10)	0.0154 (9)	0.0171 (9)	0.0028 (7)	0.0009 (7)	0.0000 (7)
C9	0.0186 (9)	0.0192 (9)	0.0149 (9)	0.0011 (7)	−0.0012 (7)	−0.0019 (7)
C10	0.0178 (9)	0.0148 (9)	0.0185 (9)	−0.0003 (7)	0.0016 (7)	−0.0013 (7)
C11	0.0204 (10)	0.0146 (9)	0.0185 (10)	0.0037 (7)	−0.0004 (8)	0.0013 (7)
C12	0.0175 (9)	0.0169 (9)	0.0184 (10)	0.0010 (7)	−0.0001 (7)	0.0001 (7)
C13	0.0194 (9)	0.0150 (9)	0.0196 (10)	0.0000 (7)	0.0013 (7)	−0.0018 (7)
C14	0.0206 (9)	0.0164 (9)	0.0214 (10)	0.0021 (7)	−0.0010 (8)	0.0016 (8)
C15	0.0226 (10)	0.0166 (9)	0.0176 (9)	−0.0001 (7)	0.0000 (8)	−0.0015 (7)
C16	0.0199 (10)	0.0162 (9)	0.0186 (10)	−0.0001 (7)	−0.0001 (8)	0.0002 (7)

Geometric parameters (\AA , $^\circ$)

O1—C7	1.227 (2)	O3—C14	1.250 (2)
N1—C2	1.340 (3)	O4—C15	1.206 (2)
N1—C1	1.348 (3)	O5—C15	1.320 (2)
N1—H1N	0.892 (10)	O5—H5O	0.848 (10)
N2—C7	1.335 (3)	O6—C16	1.229 (2)
N2—C6	1.450 (2)	O7—C16	1.315 (2)
N2—H2N	0.878 (10)	O7—H7O	0.847 (10)
C1—C5	1.384 (3)	C8—C13	1.387 (3)
C1—C6	1.504 (3)	C8—C9	1.393 (3)
C2—C3	1.377 (3)	C8—C14	1.516 (3)
C2—H2	0.9500	C9—C10	1.395 (3)
C3—C4	1.384 (3)	C9—H9	0.9500
C3—H3	0.9500	C10—C11	1.385 (3)
C4—C5	1.385 (3)	C10—C15	1.496 (3)
C4—H4	0.9500	C11—C12	1.388 (3)
C5—H5	0.9500	C11—H11	0.9500
C6—H6A	0.9900	C12—C13	1.394 (3)

C6—H6B	0.9900	C12—C16	1.481 (3)
C7—C7 ⁱ	1.538 (4)	C13—H13	0.9500
O2—C14	1.259 (2)		
C2—N1—C1	122.36 (17)	C15—O5—H5O	110.7 (18)
C2—N1—H1N	116.1 (15)	C16—O7—H7O	107.8 (17)
C1—N1—H1N	121.5 (15)	C13—C8—C9	119.82 (17)
C7—N2—C6	122.43 (17)	C13—C8—C14	120.39 (17)
C7—N2—H2N	122.4 (15)	C9—C8—C14	119.77 (17)
C6—N2—H2N	114.8 (15)	C8—C9—C10	120.28 (17)
N1—C1—C5	118.93 (18)	C8—C9—H9	119.9
N1—C1—C6	119.35 (17)	C10—C9—H9	119.9
C5—C1—C6	121.71 (18)	C11—C10—C9	119.56 (17)
N1—C2—C3	120.45 (19)	C11—C10—C15	121.15 (17)
N1—C2—H2	119.8	C9—C10—C15	119.29 (17)
C3—C2—H2	119.8	C10—C11—C12	120.34 (17)
C2—C3—C4	118.52 (19)	C10—C11—H11	119.8
C2—C3—H3	120.7	C12—C11—H11	119.8
C4—C3—H3	120.7	C11—C12—C13	120.10 (17)
C3—C4—C5	120.13 (19)	C11—C12—C16	117.97 (16)
C3—C4—H4	119.9	C13—C12—C16	121.92 (17)
C5—C4—H4	119.9	C8—C13—C12	119.89 (17)
C1—C5—C4	119.44 (19)	C8—C13—H13	120.1
C1—C5—H5	120.3	C12—C13—H13	120.1
C4—C5—H5	120.3	O3—C14—O2	127.13 (18)
N2—C6—C1	112.55 (17)	O3—C14—C8	116.59 (17)
N2—C6—H6A	109.1	O2—C14—C8	116.27 (17)
C1—C6—H6A	109.1	O4—C15—O5	124.63 (17)
N2—C6—H6B	109.1	O4—C15—C10	122.39 (17)
C1—C6—H6B	109.1	O5—C15—C10	112.98 (16)
H6A—C6—H6B	107.8	O6—C16—O7	123.05 (17)
O1—C7—N2	125.63 (19)	O6—C16—C12	121.29 (17)
O1—C7—C7 ⁱ	121.6 (2)	O7—C16—C12	115.66 (16)
N2—C7—C7 ⁱ	112.8 (2)		
C2—N1—C1—C5	4.2 (3)	C10—C11—C12—C13	1.0 (3)
C2—N1—C1—C6	−174.80 (18)	C10—C11—C12—C16	−179.31 (17)
C1—N1—C2—C3	−1.2 (3)	C9—C8—C13—C12	1.0 (3)
N1—C2—C3—C4	−2.4 (3)	C14—C8—C13—C12	−177.46 (18)
C2—C3—C4—C5	2.9 (3)	C11—C12—C13—C8	−1.4 (3)
N1—C1—C5—C4	−3.5 (3)	C16—C12—C13—C8	178.90 (18)
C6—C1—C5—C4	175.42 (18)	C13—C8—C14—O3	−165.39 (18)
C3—C4—C5—C1	0.0 (3)	C9—C8—C14—O3	16.1 (3)
C7—N2—C6—C1	−125.7 (2)	C13—C8—C14—O2	15.3 (3)
N1—C1—C6—N2	34.8 (2)	C9—C8—C14—O2	−163.19 (18)
C5—C1—C6—N2	−144.13 (19)	C11—C10—C15—O4	−163.64 (19)
C6—N2—C7—O1	−1.8 (3)	C9—C10—C15—O4	16.4 (3)
C6—N2—C7—C7 ⁱ	179.1 (2)	C11—C10—C15—O5	16.2 (3)

C13—C8—C9—C10	−0.2 (3)	C9—C10—C15—O5	−163.84 (17)
C14—C8—C9—C10	178.26 (17)	C11—C12—C16—O6	2.0 (3)
C8—C9—C10—C11	−0.2 (3)	C13—C12—C16—O6	−178.26 (18)
C8—C9—C10—C15	179.80 (17)	C11—C12—C16—O7	−178.40 (17)
C9—C10—C11—C12	−0.2 (3)	C13—C12—C16—O7	1.3 (3)
C15—C10—C11—C12	179.82 (18)		

Symmetry code: (i) $-x, -y+1, -z+1$.

Hydrogen-bond geometry (\AA , $^\circ$)

$D\cdots H\cdots A$	$D\cdots H$	$H\cdots A$	$D\cdots A$	$D-H\cdots A$
N2—H2N \cdots O1 ⁱ	0.88 (2)	2.38 (2)	2.704 (2)	102 (1)
O7—H7O \cdots O6 ⁱⁱ	0.85 (2)	1.77 (2)	2.614 (2)	178 (2)
O5—H5O \cdots O2 ⁱⁱⁱ	0.85 (2)	1.69 (2)	2.5352 (19)	175 (2)
N2—H2N \cdots O1 ^{iv}	0.88 (2)	2.01 (2)	2.816 (2)	153 (2)
N1—H1N \cdots O3 ^v	0.89 (2)	1.73 (2)	2.604 (2)	169 (2)
C5—H5 \cdots O4 ^{vi}	0.95	2.46	3.019 (3)	117
C6—H6A \cdots O4 ^{vi}	0.99	2.55	3.362 (3)	140
C2—H2 \cdots O2 ⁱ	0.95	2.50	3.251 (3)	136
C3—H3 \cdots O6 ^{vii}	0.95	2.59	3.068 (2)	112

Symmetry codes: (i) $-x, -y+1, -z+1$; (ii) $-x, -y+1, -z$; (iii) $-x+2, y+1/2, -z+1/2$; (iv) $x-1, y, z$; (v) $-x+1, -y+1, -z+1$; (vi) $x-2, y, z$; (vii) $x-1, -y+3/2, z+1/2$.